

Application of magnetic atom induced bound states in superconducting gap for chemical identification of single magnetic atoms

Shuai-Hua Ji,^{1,2} Tong Zhang,^{1,2} Ying-Shuang Fu,^{1,2} Xi Chen,² Jin-Feng Jia,² Qi-Kun Xue,^{1,2} and Xu-Cun Ma^{1,a)}

¹*Institute of Physics, Chinese Academy of Sciences, Beijing 100190, People's Republic of China*

²*Department of Physics, Tsinghua University, Beijing 100084, People's Republic of China*

(Received 4 December 2009; accepted 24 January 2010; published online 18 February 2010)

Elemental identification at single atom level has been achieved with a low temperature scanning tunneling microscope. Magnetic atoms (Mn or Cr) adsorbed on a superconducting Pb substrate induce a set of well-defined resonance states inside the superconductor gap in scanning tunneling spectroscopy. We show that these localized characteristic bound states could serve as fingerprint for chemical identification of the corresponding atoms, similar to atomic/molecular spectra widely used in optical spectrometry. The experiment demonstrates a technique for element-resolved spectroscopy with simultaneous atomic-level spatial resolution. The influence of magnetic impurity concentration on the bound states has also been investigated. © 2010 American Institute of Physics. [doi:10.1063/1.3318404]

Elemental identification at single atomic/molecular level¹⁻⁵ is one of the ultimate goals in developing various microscopic techniques including scanning tunneling microscopy (STM). STM can resolve surface structure with real-space atomic resolution but cannot directly offer the chemical identity of an atom or molecule without additional inputs from scanning tunneling spectroscopy (STS). A major breakthrough in this field is the development of inelastic electron tunneling spectroscopy,¹ by which one can simultaneously image and identify a single molecule on a surface through measurement of the vibrational excitation of chemical bonds in the molecule. However, similar capability remains to be developed for obtaining explicit “fingerprint” of single atoms.

The obstacle to elemental identification of an atom by STM lies in the fact that chemical sensitivity could not be readily reached by the primitive electronic structure measurement, which covers only a few electron volt in energy around the Fermi level. Upon adsorption, the outermost *s* or *p* electrons of an atom are highly hybridized with the conduction band of the substrate. The resulting electronic structure, which can be probed by STS when the STM tip is above the adsorbed atom, is more or less featureless and provides no chemical identification capability. The less hybridized *d* or *f* orbitals of a metal atom, which carry element specific information, are either too localized or too far below the Fermi level to be resolved in STS. These difficulties lead us to consider another degree of freedom of an atom, i.e., the spin of electrons.

In this letter, we report on STM identification of individual transition metal (Mn and Cr) atoms adsorbed on the surface of superconducting Pb films by using their characteristic resonance states induced by the coupling between the localized spin and the superconducting electrons.⁶⁻⁹ The low energy bound states induced by single Mn or Cr atoms have been reported in a previous study.¹⁰ Here we show that these spatially well-localized bound states can be used as the fingerprints to spectroscopically identify single atoms.

Our experiments were conducted with a Unisoku UHV He3-STM system with the base pressure of 1×10^{-10} Torr. The energy resolution of STS in this system is better than 0.1 meV.¹⁰ Pb (99.999%) was deposited on the clean Si(111)-7 \times 7 reconstruction surface at room temperature with additional annealing for 30 min at the same temperature to form uniform Pb film. In this study, we used the 20 ML film as the substrate. The thickness was determined by the characteristic quantum well states.¹¹⁻¹³ The superconducting gap Δ_{sample} of the film is 1.30 meV compared with 1.55 meV for bulk Pb. Mn (99.98%) or Cr (99.999%) atoms were deposited on the Pb substrate at a temperature of 30 K. To enhance the sensitivity and signal-to-noise ratio of STS, a superconducting Nb tip with a gap of $\Delta_{\text{tip}}=1.52$ meV was used. Therefore, the differential conduction dI/dV is the convolution of two BCS-type density of states. In the experiments, dI/dV was measured by lock-in technique with a modulation voltage of 0.05 mV at 1.991 KHz.

Figures 1(a) and 1(b) show the topographic image of a single Mn atom on the Pb film and the differential conductance dI/dV measured at various locations. The electronlike and holelike bound states are clearly resolved.¹⁰ With increasing distance from the atom, the bound states fade away rapidly. After numerical deconvolution of each curve in Fig. 1(b) to remove the density of states of the tip, we obtained the spatial distribution [Fig. 1(c)] of the bound states as a function of the distance to the center of Mn atom. The bound states are highly localized around the Mn atom. Similar behavior has been observed for Cr atoms deposited on Pb, whose bound states appear at different energies than those of Mn.

The element-dependent localized bound states offer an opportunity to identify the species of single atoms by STM. To demonstrate this, we simultaneously deposited Mn and Cr atoms on the Pb film. The adsorbed Mn and Cr atoms distribute randomly on the surface, as shown in the STM image in Fig. 2(a) and the schematic in Fig. 2(b). In the usual constant-current topographic image, the seven atoms in Fig. 2(a) exhibit similar contrast and are not distinguishable. When the spatial distribution of dI/dV at fixed bias of 1.77

^{a)}Electronic mail: xcma@aphy.iphy.ac.cn.

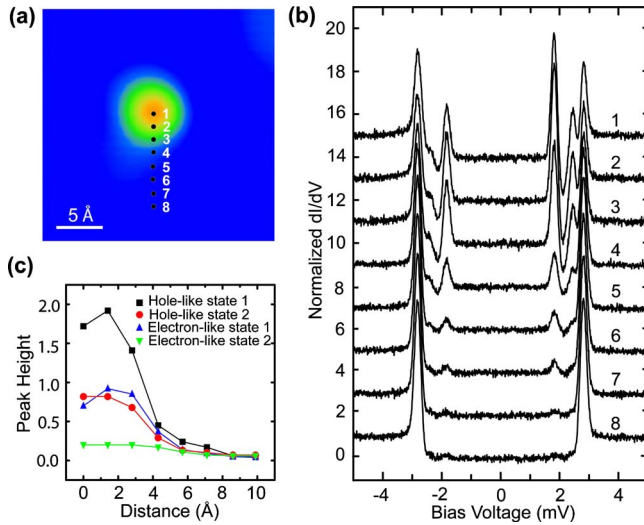


FIG. 1. (Color online) (a) STM image ($2.5 \times 2.5 \text{ nm}^2$) of an Mn atom showing eight points where the dI/dV spectra in (b) were recorded. Tunneling conditions: $V=20 \text{ mV}$ and $I=0.1 \text{ nA}$. (b) Normalized dI/dV spectra at eight different locations around the Mn atom. Tunneling conditions: $V=10 \text{ mV}$ and $I=0.2 \text{ nA}$. The curves were offset for clarity. (c) The intensity of each component of the bound states as a function of the distance from the atom. The intensities were obtained by the numerical deconvolution of dI/dV curves in (b).

mV (corresponding to one of the electronlike bound state induced by Mn) and -2.39 mV (corresponding to one of the holelike bound state induced by Cr) were recorded, respectively, for the same area as in Fig. 2(a), the locations of the Mn atoms [Fig. 2(c)] and those of the Cr atoms [Fig. 2(e)] were clearly revealed. The spatial extent of the gap states appears to be as narrow as the constant-current atomic images. We further note that the spectra from the same type of atom are very reproducible [see the different curves in Fig. 2(d) for Mn, and those in Fig. 2(f) for Cr], suggesting that

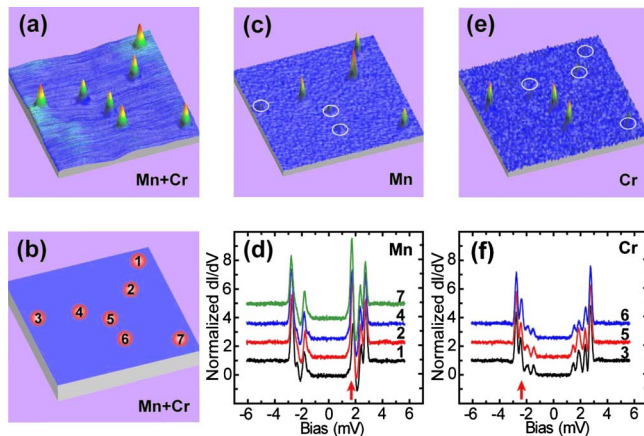


FIG. 2. (Color online) (a) Topographic image of an area with codeposited Mn and Cr atoms at a total coverage of 0.001 ML on the Pb film. The seven atoms were seen as round protrusions. Imaging conditions: 2.0 V bias and 0.1 nA tunneling current. (b) The schematic of (a). (c) dI/dV mapping of the same area as in (a). It was acquired with 1.77 mV bias voltage which is the position of one of the electronlike bound states for Mn atoms. The mapping exclusively shows the locations of Mn out of the seven atoms. (d) dI/dV spectra obtained on atom 1, 2, 4, and 7. (e) dI/dV mapping acquired with 2.10 mV bias voltage which is the position of one of the holelike bound states of Cr atoms. Only Cr atoms show up in the mapping. (f) dI/dV spectra obtained on atom 3, 5, and 6. The curves in [(d) and (f)] were offset vertically for clear display. The open circles in [(c) and (e)] indicate the positions of the invisible Cr or Mn atoms in each mapping.

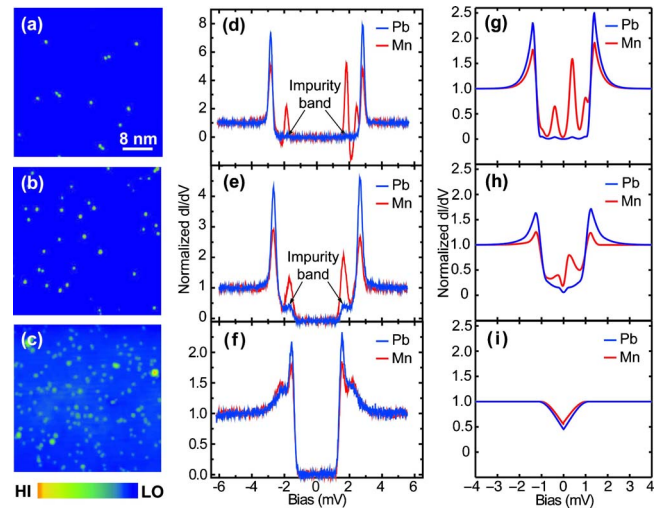


FIG. 3. (Color online) [(a)–(c)] Topographic images of Pb film surface with different Mn impurity density. [(d)–(f)] The corresponding dI/dV spectra on the top of Mn atoms (red curves) and the Pb film (blue curves). [(g)–(i)] The normalized dI/dV after removing the tip effect on the spectra. The red curves are on the top of Mn atoms and the blue curves on the Pb film.

these bound states and their unique energies are indeed the fingerprint of a magnetic atom, in a similar way as the vibrational frequencies which are intrinsic to a molecule.¹

In the above approach, the capability of STS to resolve elements depends on both the energy resolution of the instrument and the peak width of the bound states. Usually, the peak width is much less than the typical separation ($\sim 0.1 \text{ meV}$) between two bound states. Thus different bound states can be clearly resolved by STS. However, if the coverage of magnetic atoms is increased, the bound states of different atoms will spatially overlap and eventually form the impurity bands.^{9,14–20} Therefore, at higher coverage the STS loses the capability to identify the species of individual atoms by the spin-induced bound states in superconducting gap. Figures 3(a)–3(c) show the STM images obtained on the Pb film surface covered with different densities of Mn atoms. While most adsorbates in Fig. 3(a) ($\sim 0.00082 \text{ ML}$ coverage) and Fig. 3(b) (0.0026 ML) remain as single atoms; clusters of different sizes are formed when the Mn coverage increases to 0.014 ML [Fig. 3(c)]. The dI/dV spectra in Figs. 3(d)–3(f) are the tunneling conductance at different coverage measured with a Nb tip at 0.4 K. The density of states of the surface was extracted from the spectra by numerical deconvolution as shown in Figs. 3(g)–3(i). The bound states develop into impurity bands with increasing coverage. At the same time the coherence peaks (also the superconductivity order parameter) are greatly reduced at high density of magnetic impurities. As a result, the capability of chemical identification by STS is attenuated.

In summary, both elemental identification and atomic resolution are achieved simultaneously in this study. In addition to its high sensitivity, this element-resolved single atom spectroscopy can be applied to various elements, ranging from transition metals to rare earths. The substrate is not necessarily to be Pb as long as the local magnetic moment of the atom is not quenched and can create bound states in the superconducting gap. Furthermore, a superconductor may induce pairing correlations in a normal metal due to the proximity effect. Therefore, the element-resolved spectroscopy can be extended to the surface of normal metal films grown

on a superconductor in order to study coordination chemistry at the single molecular level.²¹

This work was supported by National Natural Science Foundation of China and the Ministry of Science and Technology of China. The STM topographic images were processed using WSxM (www.nanotec.es).

¹B. C. Stipe, M. A. Rezaei, and W. Ho, *Science* **280**, 1732 (1998).

²K. Suenaga, M. Tencé, C. Mory, C. Colliex, H. Kato, T. Okazaki, H. Shinohara, K. Hirahara, S. Bandow, and S. Iijima, *Science* **290**, 2280 (2000).

³T. Eguchi, T. Okuda, T. Matsushima, A. Kataoka, A. Harasawa, K. Akiyama, T. Kinoshita, Y. Hasegawa, M. Kawamori, Y. Haruyama, and S. Matsui, *Appl. Phys. Lett.* **89**, 243119 (2006).

⁴Y. Sugimoto, P. Pou, M. Abe, P. Jelinek, R. Pérez, S. Morita, and Ó. Custance, *Nature (London)* **446**, 64 (2007).

⁵D. A. Muller, L. F. Kourkoutis, M. Murfitt, J. H. Song, H. Y. Hwang, J. Silcox, N. Dellby, and O. L. Krivanek, *Science* **319**, 1073 (2008).

⁶A. Yazdani, B. A. Jones, C. P. Lutz, M. F. Crommie, and D. M. Eigler, *Science* **275**, 1767 (1997).

⁷M. E. Flatté and J. M. Byers, *Phys. Rev. Lett.* **78**, 3761 (1997).

⁸M. I. Salkola, A. V. Balatsky, and J. R. Schrieffer, *Phys. Rev. B* **55**, 12648 (1997).

⁹A. V. Balatsky, I. Vekhter, and J.-X. Zhu, *Rev. Mod. Phys.* **78**, 373 (2006).

¹⁰S.-H. Ji, T. Zhang, Y.-S. Fu, X. Chen, X.-C. Ma, J. Li, W.-H. Duan, J.-F. Jia, and Q.-K. Xue, *Phys. Rev. Lett.* **100**, 226801 (2008).

¹¹X.-C. Ma, P. Jiang, Y. Qi, J.-F. Jia, Y. Yang, W.-H. Duan, W.-X. Li, X. Bao, S. B. Zhang, and Q.-K. Xue, *Proc. Natl. Acad. Sci. U.S.A.* **104**, 9204 (2007).

¹²Y.-S. Fu, S.-H. Ji, X. Chen, X.-C. Ma, R. Wu, C.-C. Wang, W.-H. Duan, X.-H. Qiu, B. Sun, P. Zhang, J.-F. Jia, and Q.-K. Xue, *Phys. Rev. Lett.* **99**, 256601 (2007).

¹³Y. Qi, X.-C. Ma, P. Jiang, S. Ji, Y. Fu, J.-F. Jia, Q.-K. Xue, and S. B. Zhang, *Appl. Phys. Lett.* **90**, 013109 (2007).

¹⁴H. Shiba, *Prog. Theor. Phys.* **40**, 435 (1968).

¹⁵L. Dumoulin, E. Guyon, and P. Nedellec, *Phys. Rev. Lett.* **34**, 264 (1975).

¹⁶L. Dumoulin, E. Guyon, and P. Nedellec, *Phys. Rev. B* **16**, 1086 (1977).

¹⁷J. K. Tsang and D. M. Ginsberg, *Phys. Rev. B* **22**, 4280 (1980).

¹⁸W. Bauriedl, P. Ziemann, and W. Buckel, *Phys. Rev. Lett.* **47**, 1163 (1981).

¹⁹A. A. Abrikosov and L. P. Gor'kov, *Zh. Eksp. Teor. Fiz.* **39**, 1781 (1960) [*Sov. Phys. JETP* **12**, 1243 (1961)].

²⁰M. A. Woolf and F. Reif, *Phys. Rev.* **137**, A557 (1965).

²¹W. Ho, *J. Chem. Phys.* **117**, 11033 (2002).